

Scaling Properties of Branched Polyesters. 2. Static Scaling above the Gel Point

Ralph H. Colby* and Michael Rubinstein

Corporate Research Laboratories, Eastman Kodak Company,
Rochester, New York 14650-2110

Jeffrey R. Gillmor and Thomas H. Mourey

Analytical Technology Division, Research Laboratories, Eastman Kodak Company,
Rochester, New York 14650-2136

Received July 27, 1992

ABSTRACT: We report experimental data on gel fraction, gel equilibrium swelling, sol intrinsic viscosity, and molecular weight distribution of the sol for a series of polyester samples above the gel point. The data are analyzed in terms of scaling relations suggested by percolation theory. We determine the Fisher exponent τ that describes the power law distribution of molecular weights at the gel point, by five independent methods above the gel point, and conclude $\tau = 2.35 \pm 0.03$ (95%). This is in excellent agreement with the previously reported analysis of τ below the gel point for the same polyester system. The measured τ is intermediate between the expectations of three-dimensional percolation theory ($\tau = 2.2$) and the mean-field Flory-Stockmayer theory ($\tau = 2.5$). We interpret the intermediate exponent in terms of a crossover between the two limiting theories and estimate the prefactor for the Ginzburg criterion from the experimental data. We also find that network strands are not able to completely disintersperse when the network is swollen in a good solvent.

Introduction

Gelation is one of the oldest and most important problems in polymer science.¹ The mean-field theory of Flory^{1,2} and Stockmayer³ is now 50 years old, but three-dimensional percolation views of gelation^{4,5} and the crossover between the two models⁶⁻⁸ have only developed over the last 15 years. Experimental data prior to 1982 are interpreted in light of these theories in the review by Stauffer et al.⁹ Recently, a number of excellent experimental works¹⁰⁻³³ have demonstrated the utility of the scaling ideas that emerge from the two models, but experimentally determined values of the scaling exponents are often found to fall between the values predicted by the two theories. These studies focused primarily on characterization of branched polymers below (but near) the gel point, as was the case for the previous paper from these laboratories on branched polyesters.²⁴ Only four recent studies have characterized samples beyond the gel point^{10,17,20,25} and the data are somewhat inconclusive.

In this paper we present characterization results on a branched polyester system beyond the gel point, and compare the resulting scaling exponents with those obtained for the same polymer system below the gel point.²⁴ This system has the unique advantage of reaction proceeding at elevated temperatures by an ester-exchange reaction that allows the gel structure to equilibrate, thereby maintaining ergodicity. At the elevated temperatures required for reaction (180–240 °C), the reaction is reversible and thus the system is able to sample many possible configurations beyond the gel point. Our system is, therefore, more suitable than most for testing equilibrium theories. The reaction is conveniently stopped by cooling to room temperature.

We also report, for the first time, the equilibrium swelling of the gel fraction of near-critical gels and compare it with recent scaling predictions. From these measurements, we find conclusive evidence that network strands cannot fully disintersperse upon swelling.

Background Theory

As discussed by Stauffer,^{9,34} both the mean-field Flory-Stockmayer theory and the three-dimensional percolation

theory predict scaling relations among various quantities near the gel point. The main differences in predictions of the theories are in the numerical values of the scaling exponents. In fact, each of the theories applies to different experimental situations, referred to as universality classes. In this section we introduce the scaling relations we will need in this study and simply summarize the predictions of the exponents in Table I for the two universality classes (mean field and 3D percolation).

The molecular weight distribution, described by $n(M)$, the number density of molecules with mass M , is a power law in M that is truncated at high molecular weight by a cutoff function $f(M/M_{\text{char}})$.

$$n(M) = M^{-\tau} f(M/M_{\text{char}}) \quad (1)$$

The characteristic largest molecular weight, M_{char} , diverges with exponent $1/\sigma$, as the gel point is approached from either side.

$$M_{\text{char}} \sim |p - p_c|^{-1/\sigma} \quad (2)$$

Here, p is the extent of reaction (fraction of all possible bonds that have formed) and p_c is the critical extent of reaction (gel point). Thus, the molecular weight distribution becomes infinitely broad at the gel point.

A number of measurable quantities are defined as moments of the molecular weight distribution. The k th moment of the distribution is defined in the usual way.

$$m_k = \sum_M M^k n(M) \sim |p - p_c|^{(\tau-k-1)/\sigma} \quad (3)$$

Equations 1–3 apply on both sides of the gel point, with the implicit provisos that we only treat the sol fraction above the gel point and that the cutoff function may be different on the two sides of the phase transition.³⁴

The first moment m_1 scales as the sol fraction. It is constant below the gel point and decreases above the gel point as mass is incorporated into the gel fraction ($m_1 \sim 1 - P_{\text{gel}}$). The gel fraction P_{gel} is the order parameter for this phase transition³⁴ (zero below the gel point and nonzero above) and grows beyond the gel point with exponent β .

$$P_{\text{gel}} \sim (p - p_c)^\beta \quad p > p_c \quad (4)$$

The exponent β is related to τ and σ through a scaling relation (from the $k = 1$ case of eq 3).

$$\beta = (\tau - 2)/\sigma \quad (5)$$

The ratio of second and first moments defines the weight-average molecular weight $M_w = m_2/m_1$, which diverges with exponent γ as the gel point is approached from either side.

$$M_w \sim |p - p_c|^{-\gamma} \quad (6)$$

Another scaling relation links γ to τ and σ (from the $k = 2$ case of eq 3).

$$\gamma = (3 - \tau)/\sigma \quad (7)$$

Higher order mass averages such as $M_z = m_3/m_2$ all diverge in the same manner as the characteristic molecular weight M_{char} (see eq 2), because ratios of m_k/m_{k-1} scale as $|p - p_c|^{-1/\sigma}$ for $k \geq 3$ (see eq 3; this is a direct consequence of $2 < \tau < 3$).

Spectroscopic techniques typically measure the extent of reaction, with a relative error of ca. $\pm 5\%$. Regardless of the magnitude of this error, the uncertainty in $p - p_c$ diverges at the gel point. Therefore, we are motivated to compare two quantities that are more precisely measurable near the gel point and thereby evaluate a ratio of critical exponents.

$$M_{\text{char}} \sim M_w^{1/\sigma\gamma} \sim M_w^{1/(3-\tau)} \quad (8)$$

$$P_{\text{gel}} \sim M_w^{-\beta/\gamma} \sim M_w^{-(\tau-2)/(3-\tau)} \quad (9)$$

Both eqs 8 and 9 effectively provide another measure of the exponent τ .

The equilibrium swelling ratio Q is defined as the ratio of volumes of the gel in the fully swollen and dry states (with the sol fraction removed in each case). Daoud et al.³⁵ calculated the equilibrium swelling by assuming that network chains are free to completely disintersperse when swollen. This assumption is central to the c^* theorem of de Gennes³⁶ for network swelling. In the c^* theorem, the network strands are presumed to be just at the overlap concentration (c^*) when fully swollen (at equilibrium with pure solvent). Thus, in situations where the network strands are strongly overlapped in the unswollen state, the strands must completely disintersperse to get to c^* in the swollen state.

Daoud et al.³⁵ predicted the equilibrium swelling ratio scaling with the gel fraction

$$Q \sim P_{\text{gel}}^{-z} \quad (10)$$

with

$$z = \frac{(d/D_s) - 1}{\tau - 2} \quad (11)$$

where d is the dimension of space ($=3$) and D_s is the fractal dimension of swollen branched polymers. Theory^{37,38} predicts $D_s = 2$, and all experimental results are consistent with that prediction^{14,24,39} with specific findings of $D_s = 1.98 \pm 0.03$ ¹⁴ and $D_s = 2.04 \pm 0.04$.²⁴ In this paper we will take two approaches: We will first assume $D_s = 2$ and use swelling measurements to determine the exponent τ . Second, we will use the experimentally measured τ and z exponents to determine D_s . Originally, eq 11 was derived³⁵ using the hyperscaling relation³⁴ (only valid for percolation). However, if complete disinterspersion of network

Table I
Critical Exponent Predictions^{23,34}

	τ	σ	β	γ	$1/\sigma\gamma$	β/γ	z	a
defining eq	1	2	4	6	8	9	10	12
mean field	$5/2$	$1/2$	1	1	2	1	1	0 ^a
3D percolation	2.2	0.46	0.43	1.74	1.26	0.25	2.5	0.38

^a Logarithmic divergence.

strands on swelling is assumed, eq 11 applies to the mean-field limit as well.³⁵

Intrinsic viscosity, both above and below the gel point, is expected to be a power law in weight-average molecular weight⁴⁰

$$[\eta] \sim M_w^a \quad (12)$$

with

$$a = \frac{(d/D_s) - \tau + 1}{3 - \tau} \quad (13)$$

As in the case above for swelling, if we assume $D_s = 2$, as expected for randomly branched polymers, intrinsic viscosity provides an additional determination for τ . On the other hand, if we know τ and a , we can determine D_s . Both will be done below.

Above the gel point, the assumption of complete disinterspersion of network chains leads us to expect a very simple relation between intrinsic viscosity, equilibrium swelling ratio, and gel fraction.

$$[\eta] \sim QP_{\text{gel}} \quad (14)$$

The physical significance of the product QP_{gel} is the ratio of the swollen gel volume to the total sample volume in the reaction bath (sol plus gel). We will demonstrate that eq 14 is not obeyed for our data and attribute the deviation to a breakdown of the c^* theorem assumption for all networks that are not in the percolation universality class. Hyperscaling³⁴ requires strands of percolation networks to not be strongly overlapping, whereas the mean-field limit corresponds to strong overlap of network strands. Apparently, overlap prevents the network strands from completely disinterspersing to c^* when swollen.

The predictions of the two models for the various exponents defined above are summarized in Table I. Clearly, a correlation of gel fraction and weight-average molecular weight will provide the best means of distinguishing between the two theories, as the exponent of eq 9 has the largest relative difference in predictions.⁴¹

Recent theory⁶⁻⁸ expects each model to apply under different circumstances. Cross-linking of small multifunctional monomers should be described by three-dimensional percolation. The Flory-Stockmayer theory models cross-linking of a melt of long, strongly overlapping, linear chains. De Gennes⁶ refers to this class as vulcanization.

Real gelation reactions usually correspond to situations that are somewhere between these two extremes. Close to the gel point the three-dimensional percolation model is valid. Further from the gel point the mean-field model applies. The crossover has been discussed in the form of a Ginzburg criterion,⁶⁻⁸ where N is the average number of monomers between branch points.

$$\epsilon_x \equiv \frac{|p_x - p_c|}{p_c} \sim N^{-1/3} \quad (15)$$

For $\epsilon \equiv |p - p_c|/p_c \ll \epsilon_x$, the three-dimensional percolation model applies, and for $\epsilon \gg \epsilon_x$ the Flory-Stockmayer model holds (vulcanization class). The Ginzburg criterion (eq 15) predicts a crossover at a relative extent of reaction

that depends on the extent of overlap of strands between cross-links. For very large N (cross-linking of long, linear chains), ϵ_x is very small, making the entire experimentally accessible range of ϵ fall in the vulcanization class. For N of order unity (cross-linking of monomers), ϵ_x is large and the three-dimensional percolation theory should apply. However, many real systems (including the one studied here) have intermediate N . These systems should exhibit percolation exponents close to the gel point and mean-field exponents far from the gel point. Of course, eq 15 is an untested scaling relation, so the prefactor needs to be determined in order to be useful. This will be crudely attempted for our data in this paper.

Experimental Section

Synthesis. The precursor polymer was prepared via the melt condensation chemistry described in ref 24 (kindly provided by John C. Wilson), and designed to have the following molar compositions: terephthalate (0.95), glutarate (0.05), neopentyl glycol (0.90), and pentaerythritol (0.05). The second diester (glutarate) was used to prevent crystallization. The precursor polymer is below the gel point, with a weight-average molecular weight (by SEC, see below) of $M_w = 420\,000$. All samples were made from this precursor polymer via additional reaction at elevated temperature (180 °C or higher). The reaction proceeds by ester exchange, resulting in neopentyl glycol (NPG) being evolved. NMR results⁴² indicate the tetrafunctionally branched monomer (pentaerythritol) has equal reactivities for its first three reactions, but the fourth reaction is slower by a factor of 0.4. This should affect the extent of reaction corresponding to the gel point, but not the scaling exponents describing gelation.

Most samples (A–O) were prepared in a NPG/nitrogen atmosphere at 180 °C, for up to 624 h. The quantity of NPG was carefully chosen so that the reaction proceeded quite slowly (and controllably). Smaller quantities of NPG resulted in fast reaction rates (and inhomogeneous samples), while larger quantities of NPG actually caused the reaction to reverse. A typical synthesis is described in detail below. Roughly 40 h of reaction was required to reach the gel point. The reaction times are listed in Table II. There is a lack of reproducibility evident in Table II, as reaction time does not always correlate with molecular characteristics of the sol or gel. The origin of these variations is unknown, but they are not expected to influence the results of our study. Samples further beyond the gel point (P and Q in Table II) were prepared at 240 °C under nitrogen because the reaction at lower temperature simply proceeded too slowly.

Example: A 3.7-g sample of precursor polymer was placed on a Teflon-coated Kapton polyimide sheet in a 16 000-cm³ vacuum oven. A separate dish with 0.5 g of NPG was also placed in the vacuum oven. Vacuum was applied and then the oven was sealed at room temperature. The temperature was raised to 180 °C, which caused the polymer to flow into a roughly 2-mm-deep puddle and caused most of the NPG to evaporate (some NPG condensed on the coldest parts of the oven). When the temperature reached 150 °C, nitrogen gas was added to bring the total pressure to ~0.2 atm (to prevent bubbling). The sample was reacted for 354 h and then quenched by removing it from the vacuum oven and squeezing (by hand) between steel plates at room temperature. This resulted in sample N.

Gel Extraction. All samples were separated into sol and gel fractions via the standard technique of Soxhlet extraction,⁴³ in dichloromethane with 0.5- μ m (nominal) sintered glass filters. A time study was performed on one sample with a gel fraction of 0.314. The results of the extraction time study are presented in Table III. The apparent additional sol fraction obtained between 25 and 175 h is actually less than 0.0001. The extraction is therefore complete in 1 day, but we performed all extractions for 7 days to ensure complete removal of the sol from the gel. For a different sample, we compared the gel fractions obtained by 7 days of Soxhlet extraction with those obtained by undisturbed extraction in a 1000-mL separatory funnel for 30 days. The gel fractions from Soxhlet extraction ($P_{\text{gel}} = 0.20_6$) and undisturbed extraction ($P_{\text{gel}} = 0.24_6$) are within the experimental error of the Soxhlet extraction (see Table II and discussion below).

Roughly 0.3 g of sample was extracted, and replicate extractions resulted in variations in gel fraction well beyond the expected

Table II
Characterization Data for Sol and Gel Fractions

sample	t_R^a	P_{gel}	Q	$[\eta]^b$	M_w	M_z	M_{max}
A1	48	0.13 ₃		0.212	222 000	3 200 000	
B1	64	0.21 ₈		0.167	70 900	980 000	860 000
C1	76	0.23 ₇	96.5	0.173	57 900	660 000	680 000
C2	76	0.25 ₃	81.8	0.168	54 200	700 000	580 000
C3	76	0.26 ₃	77.6	0.170	47 200	630 000	530 000
C4	76	0.21 ₈	102.3	0.174	60 600	790 000	810 000
C5	76	0.25 ₄	81.9	0.173	47 300	490 000	550 000
D1	88	0.10 ₇		0.215	299 000	4 100 000	
D2	88	0.14 ₄		0.201	189 000	3 800 000	
E1	96	0.24 ₂	99.3	0.174	56 400	950 000	720 000
E2	96	0.27 ₅	77.5	0.166	44 900	560 000	640 000
E3	96	0.22 ₆	97.6	0.170	57 900	780 000	770 000
E4	96	0.24 ₅	86.3	0.169	49 800	430 000	600 000
F1	100	0.26 ₉	81.4	0.168	49 700	940 000	610 000
F2	100	0.29 ₁	74.4	0.171	46 400	550 000	560 000
F3	100	0.28 ₆	82.4	0.180	61 700	620 000	690 000
F4	100	0.32 ₃	47.4	0.172	48 200	520 000	390 000
F5	100	0.31 ₈	69.7	0.167	37 600	670 000	410 000
G1	116	0.31 ₀	63.0	0.157	33 600	300 000	250 000
G2	116	0.32 ₉	51.4	0.153	28 900	250 000	210 000
G3	116	0.32 ₆	54.4	0.154	33 000	260 000	250 000
G4	116	0.33 ₂	52.5	0.153	24 300	190 000	220 000
H1	120	0.42 ₅	40.2	0.156	26 500	140 000	150 000
H2	120	0.42 ₇	39.0	0.149	20 700	140 000	170 000
I1	140	0.55 ₀	23.7	0.142	14 500	68 000	97 000
J1	140	0.37 ₈	44.7	0.163	28 300	220 000	220 000
J2	140	0.39 ₂	44.8	0.160	28 300	170 000	210 000
K1	141	0.16 ₉		0.182	142 000	1 500 000	2 400 000
K2	141	0.20 ₂		0.180	91 900	1 200 000	940 000
K3	141	0.16 ₅		0.222	202 000	3 500 000	4 400 000
K4	141	0.20 ₅		0.184	142 000	2 200 000	1 800 000
K5	141	0.15 ₈	156.9	0.188	134 000	1 900 000	2 500 000
L1	186	0.34 ₄		0.149	26 300	190 000	210 000
L2	186	0.31 ₁		0.155	34 600	280 000	310 000
M1	290	0.29 ₁		0.151	35 500	620 000	260 000
M2	290	0.31 ₀		0.142	30 400	300 000	290 000
N1	354	0.41 ₃		0.138	20 400	130 000	140 000
N2	354	0.47 ₅		0.143	27 500	140 000	150 000
O1	624	0.53 ₂		0.141	23 700	200 000	150 000
O2	624	0.51 ₂		0.136	21 700	210 000	150 000
O3	624	0.51 ₁		0.140	22 800	160 000	120 000
O4	624	0.51 ₃		0.138	18 900	150 000	120 000
O5	624	0.53 ₁	22.7	0.114	12 400	37 000	32 000
O6	624	0.51 ₀	23.1	0.115	10 100	37 000	40 000
P1	c	0.90 ₃	8.86	0.111	9 300	37 000	23 000
P2	c	0.87 ₀	10.5	0.110	10 000	45 000	25 000
P3	c	0.88 ₁	8.95	0.112	8 100	37 000	23 000
P4	c	0.88 ₄	9.78	0.112	9 800	42 000	22 000
P5	c	0.90 ₀	11.3	0.109	7 500	21 000	20 000
Q1	d	0.68 ₁		0.121	11 300	42 000	40 000
Q2	d	0.73 ₃		0.124	9 400	43 000	45 000
Q3	d	0.80 ₀		0.114	14 900	52 000	21 000
Q4	d	0.76 ₉		0.131	8 500	39 000	47 000

^a Reaction time (h) at 180 °C in neopentyl glycol atmosphere.

^b Intrinsic viscosity (dL/g). ^c Reacted at 240 °C under nitrogen atmosphere for 18 h. ^d Reacted at 240 °C under nitrogen atmosphere for 22 h.

Table III
Extraction Time Study Results

extraction time (h)	extraction cycles ^a	apparent P_{gel}
2.5	10	0.415
7.5	30	0.325
25	100	0.314
75	300	0.314
175	700	0.314

^a Estimated number of times that solvent surrounding gel was replaced in extraction process based on a measured 15 min/cycle. experimental errors in mass measurement. We are uncertain of the origin of the random error in the gel fraction. We treat each determination as a separate sample in order to clearly show the experimental error in plots of our data. Sample N, for instance, had two determinations (N1 and N2 in Table II).

Following Soxhlet extraction, the isolated gel fraction was drained of free-standing solvent and weighed to obtain a swollen

gel mass (mass of gel plus solvent inside swollen gel). Then the gel fraction was dried under vacuum and weighed to obtain the dry gel mass. Dichloromethane was removed from the sol fraction by first drying in a rotary evaporator followed by drying under vacuum. By comparison of the dry gel mass and the sol mass with the original sample mass, two determinations of the gel fraction were made and averaged to obtain P_{gel} . The mean sum of calculated sol and gel fractions (for all samples) was 1.00 ± 0.03 . The swollen gel mass and the dry gel mass were used with the densities of the two components (CH_2Cl_2 density, 1.33 g/cm^3 ; polyester density, 1.20 g/cm^3) to calculate the swelling volume ratio Q . Values of gel fraction and swelling volume ratio are listed in Table II.

Size-Exclusion Chromatography. The size-exclusion apparatus utilizing low-angle laser light-scattering (LALLS), differential viscometry (DV), and differential refractive index (DRI) detection has been described previously.^{44,45} Four 10- μm PLgel mixed-bed columns (Polymer Laboratories, Amherst, MA) and a precolumn were coupled in series without a postcolumn filter. The eluent was uninhibited tetrahydrofuran (THF), pumped at a nominal flow rate of 1.00 mL/min. The retention volume of an internal standard, 1-chloro-2,4-dinitrobenzene, was used to correct for flow rate variations. All samples were prefiltered through 0.2- μm Anotop inorganic membrane filters (Alltech Associates) prior to the SEC experiment. These filters have a well-defined size cutoff that is roughly equivalent to the hydrodynamic diameter of linear polystyrene of molecular weight 8 000 000 in THF. Sample concentrations were 2–6 mg/mL, injected in a volume of 100 μL . The refractive index increment, $dn/dc = 0.134$ at 632.8 nm (required for the calculation of weight-average molecular weight from LALLS), was measured in THF at 25.0 °C. Intrinsic viscosity, $[\eta]$, and weight-average molecular weight, M_w , reported in Table II, were obtained by integrating the DV and LALLS detector responses, respectively.^{46,47} The z-average molecular weight, M_z , was obtained by summation using the molecular weight (from LALLS) and concentration (from DRI) at each retention volume. The molecular weight corresponding to the peak output from the LALLS detector, M_{max} (a measure of the cutoff molecular weight, M_{char}),^{12,23} is also reported in Table II. All data in Table II from the SEC experiment ($[\eta]$, M_w , M_z , M_{max}) are averages of between two and six replicate SEC analyses. M_{max} could not be resolved for the two samples closest to the gel point (A and D), due to the inability of our columns to adequately separate species with molecular weight M_{max} from molecules that are excluded from the column packing pores. Likewise, M_z is questionable for these samples (but still reported). Since $[\eta]$ and M_w are obtained by integrations of the DV and LALLS detector responses, their determinations do not rely on perfect separation of the high molecular weight tail, and thus we believe these results are still accurate for samples A and D.

Measurements of $[\eta]$ and M_w from integration of the LALLS and DV responses typically have standard deviations of less than $\sigma = \pm 4\%$ for broad molecular weight distribution, linear polystyrene.⁴⁴ However, for the branched polyester sols in this study, we find $\sigma([\eta]) = \pm 5\%$ and $\sigma(M_w) = \pm 12\%$. The distinction to be made between these branched sols and linear polymers is the need to cleanly separate the sol fraction from the gel by Soxhlet extraction, followed by prefiltration. A small amount of gel contamination in the sol has a relatively small effect on the calculation of $[\eta]$ by DV but greatly affects the integrated light scattering from the LALLS detector. The poorer statistics on M_w are thus attributed to the inability to reproducibly separate the last traces of gel from the sol. Higher moments of the size distribution are even more sensitive to the presence of gel, and we find $\sigma(M_z) = \pm 24\%$.

In principle, one can calculate M_w and M_z from DV detector output using universal calibration. This is tempting for analysis of sol fractions because DV is far less sensitive to gel contamination, as evidenced by the difference in reproducibility of $[\eta]$ and M_w . However, it has been shown that the local molecular weight calculated by this method is actually a number average,⁴⁸ and the average from higher moments (M_w , M_z) calculated from summation can lead to systematic errors. Therefore we only calculate $[\eta]$ from DV and calculate molecular weights from the LALLS detector, relying on a large number of samples to improve the statistics of the critical exponents we determine. It is important to recognize in the following discussion of results that

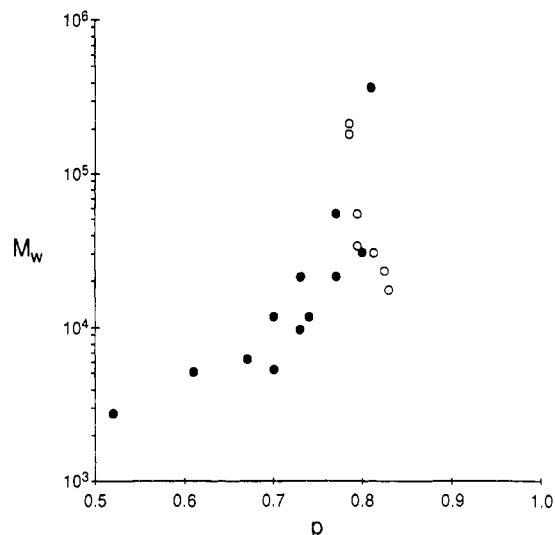


Figure 1. Weight-average molecular weight as a function of extent of reaction determined by NMR. Filled symbols are samples below the gel point.²⁴ Open symbols are sol fractions above the gel point.

the relative precision of the data decreases in the following order: $[\eta]$ ($\pm 5\%$), P_{gel} ($\pm 7\%$), M_w ($\pm 12\%$), M_{max} ($\pm 13\%$), Q ($\pm 13\%$), M_z ($\pm 24\%$).

Results

In ref 24, the extent of reaction was measured by a NMR method for polyesters below the gel point. This technique was also employed for some of the samples in this study. In Figure 1, we plot weight-average molecular weight as a function of extent of reaction, both for samples below the gel point (ref 24) and for samples above the gel point. Notice that the two sets of data overlap in the range $0.78 < p < 0.81$. Presumably the gel point (p_c) is within this range of p ; ref 24 evaluated p_c and γ from nonlinear regression fits to eq 6 and obtained $p_c = 0.84 \pm 0.07$ and $\gamma \approx 1.8 \pm 0.3$. The value of γ obtained by such a procedure is extremely sensitive to the choice for p_c . A random error in p of ca. $\pm 5\%$ translates to a minimum error in p_c of 5%, and this is simply too large to make the extent of reaction useful for accurate determination of critical exponents. We believe the problem is, in fact, a generic one for all gelation studies, not merely a specific problem for this system. Extent of reaction is typically measured by spectroscopic techniques of one form or another, which have some inherent relative uncertainty. The crucial quantity for evaluation of critical exponents is $p - p_c$ very close to p_c . Since both p and p_c have a fixed relative uncertainty, the relative uncertainty in $p - p_c$ diverges at the gel point! In order to circumvent this problem, we compare two quantities with finite random errors and evaluate ratios of exponents (see eqs 8 and 9).

We plot the gel fraction as a function of weight-average molecular weight in Figure 2. A least-squares fit to the data is shown as the solid line in Figure 2, yielding the ratio of exponents

$$\beta/\gamma = 0.56 \pm 0.04 \text{ (95\%)} \Rightarrow \tau = 2.36 \pm 0.02 \text{ (95\%)}$$

As discussed above, Figure 2 should provide the best determination of universality class, as there are large differences between β/γ predicted by the two theories (see Table I). Unfortunately, the data indicate an intermediate value of β/γ , which leads to a value of τ halfway between the predictions of percolation and mean field. There is a slight hint of curvature in Figure 2, which is consistent with the idea of a crossover between the two theories. Close to the gel point (large M_w) the apparent magnitude of the

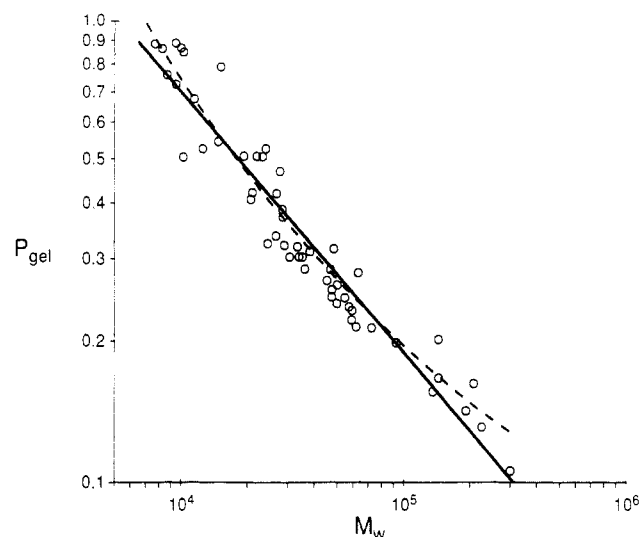


Figure 2. Correlation of gel fraction and weight-average molecular weight of the sol. Solid line is a linear regression fit to eq 9. Dashed curve is a nonlinear regression fit to eq 16.

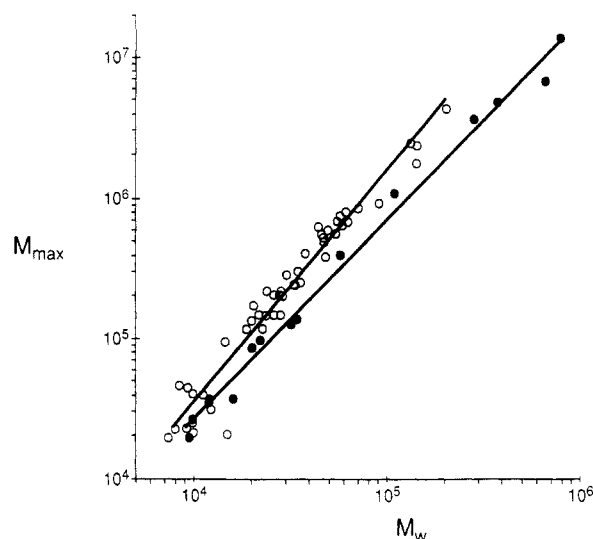


Figure 3. Correlation of molecular weight where the maximum in light-scattering intensity occurs and weight-average molecular weight. Filled symbols are samples below the gel point.²⁴ Open symbols are sol fractions above the gel point. Solid lines are linear regression fits to eq 8 for each data set, with M_{\max} replacing M_{char} .

slope decreases, consistent with the lower value anticipated for percolation ($\beta/\gamma = 0.25$). Far from the gel point (small M_w) the absolute value of the slope increases, as expected for the mean-field theory ($\beta/\gamma = 1$). We will return to this point in the Discussion section.

In Figure 3 we plot the molecular weight corresponding to the maximum in light-scattering intensity, M_{\max} , as a function of weight-average molecular weight. This plot was also made in ref 24, and we include their data below the gel point in Figure 3. Clearly, the data below and above the gel point are different, with the M_{\max} values consistently larger above the gel point (at a given M_w). This is expected because the cutoff function (eq 1) is only symmetric for the mean-field theory.³⁴ For percolation there is a peak in the cutoff function below the gel point, which is not present above the gel point.³⁴ Thus, if we compare samples above and below the gel point with the same M_{\max} , the one below the gel point will have a larger M_w due to the presence of the peak. The fact that the two sets of data are offset from one another provides further indication that the mean-field theory does not describe our data.

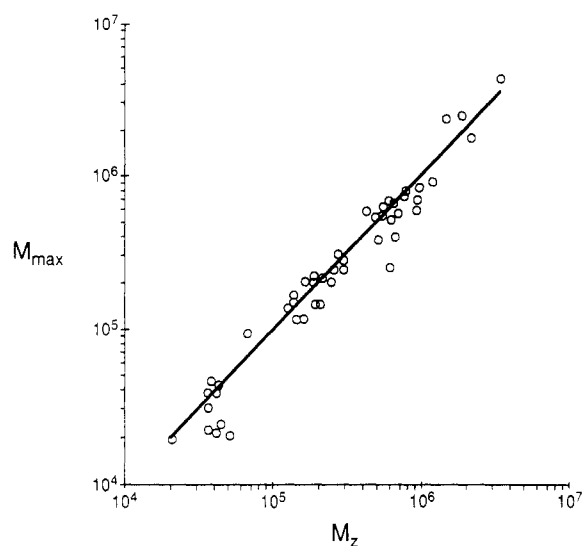


Figure 4. Correlation of molecular weight where the maximum light-scattering intensity occurs and z-average molecular weight for sol fractions. Solid line is $M_{\max} = M_z$.

Least-squares regression applied to the data in Figure 3 yields slopes of

$$1/(3 - \tau) = 1.65 \pm 0.11 \text{ (95\%)} \Rightarrow \tau = 2.39 \pm 0.04 \quad p > p_c$$

$$1/(3 - \tau) = 1.43 \pm 0.08 \text{ (95\%)} \Rightarrow \tau = 2.30 \pm 0.04 \quad p < p_c$$

The result below the gel point is from ref 24. These slopes also indicate that the apparent value of τ is intermediate between the two theoretical expectations.

We have already discussed the expectation that all molar mass averages of higher order than M_w (such as the z average, M_z) scale in the same way as the characteristic largest molecular weight M_{char} . Patton et al.²⁴ have demonstrated that the molecular weight corresponding to the maximum in the scattered light intensity, M_{\max} , also scales with M_{char} . We therefore expect M_{\max} to scale with M_z and test this assertion in Figure 4. Least-squares regression (not shown on plot) indicates a slope of 1.04 ± 0.07 (95%). We conclude that the two are indeed proportional, with $M_{\max} = 0.95M_z$.

We plot z -average molecular weight against weight-average molecular weight in Figure 5. Least-squares regression, shown as the solid line, indicates a slope of

$$1/(3 - \tau) = 1.49 \pm 0.08 \text{ (95\%)} \Rightarrow \tau = 2.33 \pm 0.04 \quad p > p_c$$

Since M_z and M_{\max} are proportional, the fact that the 95% confidence intervals on the slopes of Figures 3 and 5 overlap is an expected result.

Swelling results are plotted in Figure 6 as equilibrium swelling ratio vs gel fraction. Least-squares fitting yields the exponent

$$z = 1.70 \pm 0.07 \text{ (95\%)} \Rightarrow \tau = 2.29 \pm 0.02$$

This result for τ was obtained using eq 11, assuming $D_s = 2$ and gives further indication that τ is intermediate between the two theoretical predictions.

In Figure 7 we plot intrinsic viscosity against weight-average molecular weight. There is no apparent difference between the samples above the gel point and those below it (from ref 24). Least-squares regression applied to the data sets in Figure 7 indicates

$$a = 0.19 \pm 0.02 \text{ (95\%)} \Rightarrow \tau = 2.38 \pm 0.02 \quad p > p_c$$

$$a = 0.23 \pm 0.04 \text{ (95\%)} \Rightarrow \tau = 2.35 \pm 0.03 \quad p < p_c$$

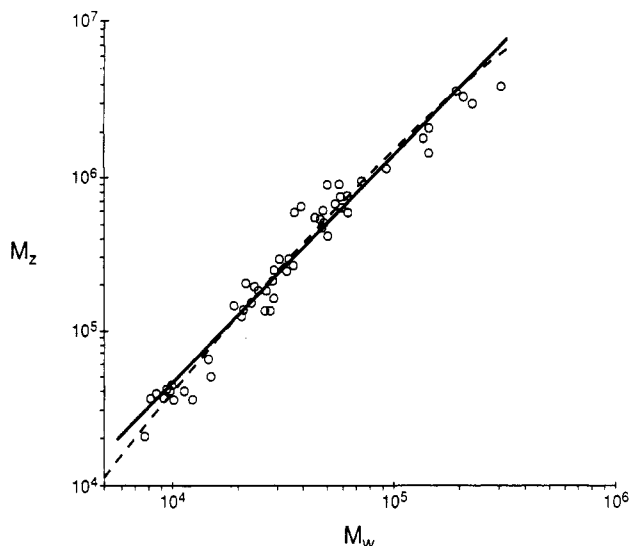


Figure 5. Correlation of z -average molecular weight and weight-average molecular weight for sol fractions. Solid line is a linear regression fit to eq 8 with M_z replacing M_{char} . Dashed curve is a nonlinear regression fit to eq 17.

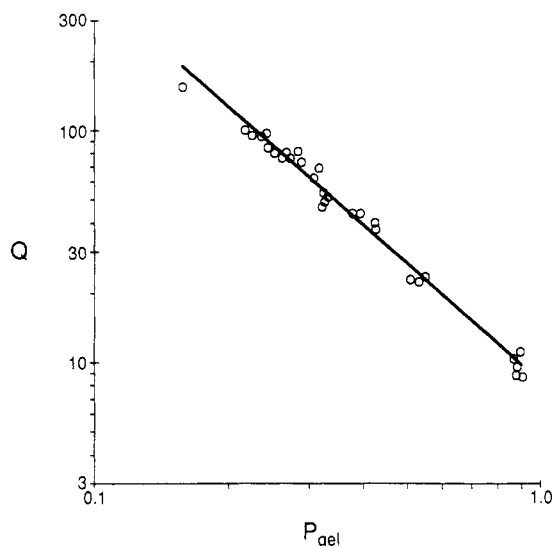


Figure 6. Correlation of equilibrium swelling ratio of the gel and gel fraction. Solid line is a linear regression fit to eq 10.

The result below the gel point is from ref 24. Both exponents agree reasonably well with the previous determinations known to us: 0.17,^{9,49} 0.30,²⁴ and 0.27.⁵⁰ The exponent τ was obtained from eq 13, assuming $D_s = 2$.

While the 95% confidence intervals for every determination of τ do not overlap, we can make some definitive conclusions. All determinations of τ are consistent with an intermediate exponent ($2.2 < \tau < 2.5$). Pooling the determinations of τ below the gel point²⁴ yields $\tau = 2.32 \pm 0.03$ (95%). Pooling the five determinations of τ above the gel point results in $\tau = 2.35 \pm 0.03$ (95%). Since there is extensive overlap of the confidence intervals for τ above and below the gel point, we can definitively conclude that a single $\tau = 2.34 \pm 0.03$ (95%) applies both above and below the gel point.

Using the pooled estimate of τ above the gel point, we can calculate the swollen fractal dimension of branched polymers (D_s) from the exponents a and z . Using eq 11 with $z = 1.70 \pm 0.07$ we find

$$D_s = 1.88 \pm 0.09 \text{ (95\%)}$$

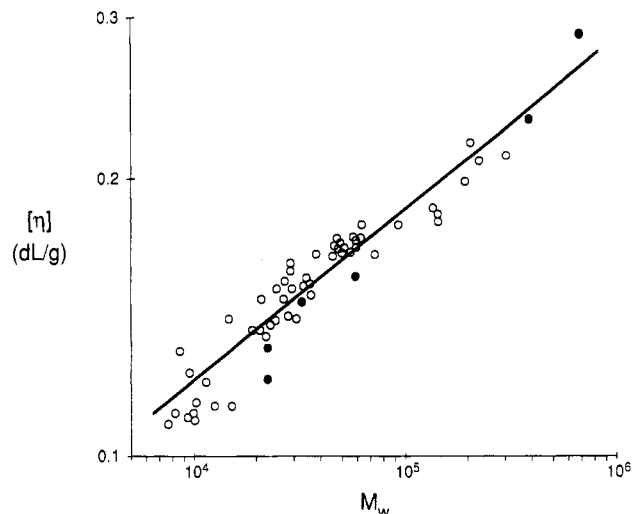


Figure 7. Correlation of intrinsic viscosity and weight-average molecular weight. Filled symbols are samples below the gel point.²⁴ Open symbols are sol fractions above the gel point. Solid line is a linear regression fit to eq 12 for sol fraction data above the gel point.

and using eq 13 with $a = 0.19 \pm 0.02$ we get

$$D_s = 2.04 \pm 0.05 \text{ (95\%)}$$

Both determinations are reasonably consistent with the expected value from theory,^{37,38} $D_s = 2$. However, the determination of D_s from swelling is significantly below the expected value of 2. We believe this is due to an invalid assumption, employed in the original derivation³⁵ of eq 11, that network strands are completely free to disintegrate upon swelling. We believe this assumption is only valid in the percolation limit.

Panyukov⁵¹ formulated a swelling prediction without this assumption. Panyukov predicted a smaller swelling than Daoud et al.³⁵ (eqs 10 and 11) because the balance between osmotic forces acting to swell the chain and entropic elasticity that restricts swelling does not allow overlapping network strands to completely disintegrate. In the mean-field limit (where network strands strongly overlap), Panyukov swelling is smaller than Daoud swelling by a factor related to the relative distance to the gel point with respect to the Ginzburg crossover ϵ_x . (Whereas in the percolation limit, where there is no overlap, the predictions are identical.) The ratio of the two predictions in the mean-field limit is

$$Q_P/Q_D = (\epsilon/\epsilon_x)^{-3/5} \quad \epsilon > \epsilon_x$$

where Q_P is the Panyukov swelling prediction⁵¹ and Q_D is the Daoud swelling prediction.³⁵ We consider the reciprocal of the swelling ratio (the polymer volume fraction in the swollen gel), as it has a very simple interpretation for the Daoud prediction in mean field.

$$1/Q_D \sim P_{gel}/[\eta] \sim p - p_c$$

The Panyukov prediction for the polymer volume fraction of the swollen gel in the mean-field limit is

$$1/Q_P \sim (p - p_c)^{8/5}$$

We plot the volume fraction of polymer in the swollen gel ($1/Q$) as a function of the ratio of gel fraction and intrinsic viscosity of the sol in Figure 8. Least-squares regression yields a slope of 1.26 ± 0.05 (95%), shown as the solid line. This clearly indicates a systematic deviation from the prediction of Daoud et al.³⁵ that leads to eq 14 (and an expected slope of unity in Figure 8). The fact that the slope is smaller than the Panyukov prediction⁵¹ of 1.6 is not surprising since our gels are in a crossover between

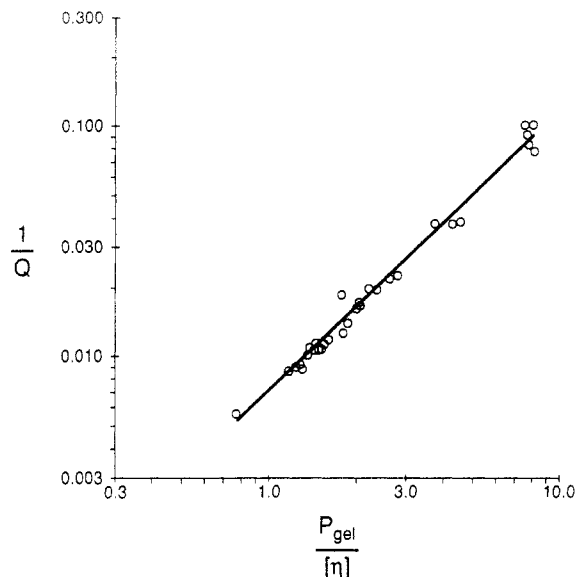


Figure 8. Correlation of reciprocal of swelling ratio of the gel with ratio of gel fraction and intrinsic viscosity of the sol (linear scales), as suggested by eq 14.

percolation and mean field, and Panyukov's result is strictly for the mean-field limit. We conclude from Figure 8 that network chains do not fully disintegrate in the swollen state. The same conclusion is already well-known for fully cured networks.⁵²

Discussion

The single most important result of both this work and ref 24 is that scaling works very nicely for describing the static characteristics of branched polymers near the gel point. In fact, scaling seems to work surprisingly far from the gel point (the lowest molecular weight branched polymers both here and in ref 24 had $M_w \approx 10\,000$, which corresponds to $P_{gel} \approx 0.75$; see Table II). Although this observation makes scaling seemingly more useful, it does point to several experimental limitations of this study. First, three-dimensional percolation is only expected to be valid very close to the gel point, whereas experimentally we can only handle samples with $M_{char} < 10^7$ due to the resolution limit of our SEC columns. This corresponds to a restriction on gel fraction $P_{gel} > 0.1$. Second, our polyester has an average degree of polymerization between branch points of $N \approx 20$, so it is not truly in either the percolation ($N \approx 1$) or vulcanization ($N \gg 1$) limits. This latter point seems to be consistent with our observation of $\tau = 2.35$, intermediate between percolation ($\tau = 2.2$) and vulcanization ($\tau = 2.5$). It seems likely that the apparent τ is really evidence for a broad crossover between the two limits. Unfortunately, we can get neither closer to nor further away from the gel point with the present system to prove this point. The best evidence we have is Figure 2, but the scatter in the data is too large to make definitive conclusions about the crossover.

The idea of a crossover in Figure 2 can be better tested by constructing a simple crossover function by addition of the two limiting power laws:

$$P_{gel} = AM_w^{-0.25} [1 + (M_w/M_x)^{-0.75}] \quad (16)$$

where A is a dimensionless parameter and M_x is the weight-average molecular weight corresponding to the center of the crossover (where the mean-field and critical contributions to P_{gel} are equal). The form of eq 16 is the simplest crossover function we can imagine that has the mean-field prediction (eq 9, with $\beta/\gamma = 1$) as its limiting behavior far from the gel point and gives the percolation prediction

(eq 9, with $\beta/\gamma = 0.25$) close to the gel point. Typical corrections to scaling in condensed matter physics often are somewhat more complicated, but similar in form.⁵³ The dashed curve in Figure 2 is the result of a nonlinear regression fit of the data to eq 16. The parameters are $A = 2.6$ and $M_x = 23\,000$. Judging from Figure 1, this (roughly) corresponds to $\epsilon_x \approx 0.04$. Since the (average) degree of polymerization between branch points is $N \approx 20$, we can estimate the prefactor for the Ginzburg criterion (eq 15) $\epsilon_x N^{1/3} \approx 0.1$. Figure 2 shows clear evidence of a broad crossover centered at $\epsilon N^{1/3} \approx 0.1$, and presumably, true mean-field exponents would only be found for $\epsilon N^{1/3} > 1$ and true percolation exponents would only be obtained for $\epsilon N^{1/3} < 0.01$. The critical regime is thus much smaller than de Gennes originally believed ($\epsilon N^{1/3} < 1$) due to the combination of a prefactor of order 0.1 and an extremely broad crossover. Perhaps this broad crossover offers some explanation for the variety of τ exponents reported in the literature that are between the two limits ($2.2 < \tau < 2.5$).

In principle the same crossover should be evident in other data as well (Figures 3 and 5–7). In practice, however, the combination of random scatter, limited data ranges, and smaller relative differences in limiting exponents makes the crossover difficult to detect. There is curvature evident in Figure 5, and we construct a crossover function as

$$M_z^{-1} = BM_w^{-1.25} [1 + (M_w/M_x)^{-0.75}] \quad (17)$$

where B is a dimensionless parameter. Equation 17 was designed to give the mean-field prediction far from the gel point (eq 8, with M_{char} replaced by M_z , and $1/\sigma\gamma = 2$) and the percolation prediction close to the gel point (eq 8, with $1/\sigma\gamma = 1.25$). In fitting data, we fix the crossover to occur at the same $M_x \approx 23\,000$ as determined in the fit to eq 16, above. In principle, the z -average molecular weight need not cross over at the same value of weight-average molecular weight as the gel fraction does, since they are determined by different moments of the molecular weight distribution. However, the combination of data scatter and small curvature in Figure 5 precludes the extraction of more than one meaningful parameter in fitting the data to eq 17. The result of a simple, single-parameter minimization of residuals fit of eq 17 to the data of Figure 5 is plotted as the dashed curve in Figure 5 (and yields $B = 0.87$). Visual inspection of Figure 5 indicates that eq 17 is not markedly different from a simple power law over the range of the data.

A major experimental concern in any study of polymers beyond the gel point is the question of whether we perfectly separate the sol and the gel. We have already discussed this as a primary source of random experimental error, but there is a potential for a systematic error here as well, particularly if the highest molecular weight species of the sol remain trapped in the gel and thus would be effectively counted as part of the gel.

Our experimental findings on melt viscoelasticity of these polyesters^{54–56} indicate that entanglements are not important in the melt, and it would be difficult to rationalize entanglements being introduced on swelling the gel. We thereby expect all of the sol to be easily removed from the gel. This assertion is further corroborated by the fact that we find the same values of τ in all experiments, both above and below the gel point.

Further evidence for complete extraction of the sol from the gel comes from Figure 3. If we were leaving the highest molecular weight species in the gel, we would expect M_{max} to be lower (at a given M_w) above the gel point than below, whereas the opposite is observed (due to the asymmetric cutoff function).

Conclusions

The static properties of branched polyesters beyond the gel point are consistent with those found below the gel point.²⁴ The scaling ideas for gelation³⁴ were found to be useful for interpreting the data. We in fact offer two data interpretations, which cannot be distinguished within our experimental error.

The first is the usual direct application of scaling to evaluate critical exponents. This resulted in multiple independent determinations of the Fisher exponent τ (defined in eq 1), which agree within experimental error, both above and below the gel point. The exponent $\tau = 2.35 \pm 0.03$ (95%) is intermediate between the theoretical values of 2.2 for three-dimensional percolation and 2.5 for the Flory-Stockmayer theory.

The second interpretation assumes that our system corresponds to a crossover between the two theories, and the data are analyzed with a simple crossover function. Fitting the data for gel fraction and weight-average molecular weight (Figure 2) to a crossover function (eq 16) enabled us to estimate the prefactor for the Ginzburg criterion for gelation.⁶ We found evidence of a broad crossover, centered around $\epsilon_r N^{1/3} \cong 0.1$. We suspect that $\epsilon_r N^{1/3} > 1$ determines where mean-field theory is valid but that true percolation exponents could only be seen in a very narrow critical region, $\epsilon_r N^{1/3} < 0.01$, due to the very broad crossover.

The crossover may explain the many intermediate critical exponents reported in the literature. Application of this crossover idea to other gelation systems is actively being pursued in our current research.

We also found that network strands do not completely disintegrate when swollen in a good solvent. This violation of the starting assumption for the c^* theorem of swelling is anticipated by the treatment of Panyukov, since our gels are in an apparent crossover between percolation (where the c^* theorem should work) and mean field (where the c^* theorem should fail). While the details of this crossover are not completely understood, one might hope that, in the future, the extent of chain interspersal in the swollen state might be used to gauge where a given gel is in the crossover.

Acknowledgment. We thank John Wilson for synthesizing the precursor polymer, Mary Goodberlet for NMR analysis of extent of reaction, and Sally Miller for assistance with the SEC experiments. We also are grateful for enlightening discussions with Mireille Adam, Mohamed Daoud, Ludwik Leibler, Francois Schosseler, and Jeffrey A. Wesson.

References and Notes

- Flory, P. J. *Principles of Polymer Chemistry*; Cornell University Press: Ithaca, NY, 1953.
- Flory, P. J. *J. Am. Chem. Soc.* **1941**, *63*, 3083, 3091, and 3096.
- Stockmayer, W. H. *J. Chem. Phys.* **1943**, *11*, 45; **1944**, *12*, 125.
- De Gennes, P. G. *J. Phys. (Paris) Lett.* **1976**, *37*, L-1.
- Stauffer, D. *J. Chem. Soc., Faraday Trans. 2* **1976**, *72*, 1354.
- De Gennes, P. G. *J. Phys. (Paris) Lett.* **1977**, *38*, L-355.
- Daoud, M. *J. Phys. (Paris) Lett.* **1979**, *40*, L-201.
- Alexander, S. In *Physics of Finely Divided Matter*; Boccardo, N., Daoud, M., Eds.; Springer: New York, 1985; p 162.
- Stauffer, D.; Coniglio, A.; Adam, M. *Adv. Polym. Sci.* **1982**, *44*, 103.
- Schmidt, M.; Burchard, W. *Macromolecules* **1981**, *14*, 370.
- Kajiwar, K.; Burchard, W.; Kowalski, M.; Neger, D.; Dusek, K.; Matejka, L.; Tuzar, Z. *Makromol. Chem.* **1984**, *185*, 2543.
- Leibler, L.; Schosseler, F. *Phys. Rev. Lett.* **1985**, *55*, 1110.
- Schosseler, F.; Leibler, L. *Macromolecules* **1985**, *18*, 398.
- Bouchaud, E.; Delsanti, M.; Adam, M.; Daoud, M.; Durand, D. *J. Phys. (Paris)* **1986**, *47*, 1273.
- Bantle, S.; Burchard, W. *Polymer* **1986**, *27*, 728.
- Adam, M.; Delsanti, M.; Munch, J. P.; Durand, D. *J. Phys. (Paris)* **1987**, *48*, 1809.
- Argyropoulos, D. S.; Berry, R. M.; Bolker, H. I. *J. Polym. Sci., Polym. Phys.* **1987**, *25*, 1191.
- Konak, C.; Tuzar, Z.; Jakes, J.; Stepanek, P.; Dusek, K. *Polym. Bull.* **1987**, *18*, 329.
- Stepanek, P.; Jakes, J.; Konak, C.; Dusek, K. *Prog. Colloid Polym. Sci.* **1988**, *78*, 72.
- Collette, C.; Lafuma, F.; Audebert, R.; Leibler, L. In *Biological and Synthetic Polymer Networks*; Kramer, O., Ed.; Elsevier: New York, 1988; p 277.
- Durand, D.; Adam, M.; Delsanti, M.; Munch, J. P. In *Universality in Condensed Matter*; Jullien, R., Peliti, L., Rammal, R., Boccardo, N., Eds.; Springer: New York, 1988; p 27.
- Delsanti, M.; Adam, M.; Munch, J. P.; Durand, D. In *Universality in Condensed Matter*; Jullien, R., Peliti, L., Rammal, R., Boccardo, N., Eds.; Springer: New York, 1988; p 35.
- Schosseler, F.; Benoit, H.; Grubisic-Gallot, Z.; Strazielle, C.; Leibler, L. *Macromolecules* **1989**, *22*, 400.
- Patton, E. V.; Wesson, J. A.; Rubinstein, M.; Wilson, J. C.; Oppenheimer, L. E. *Macromolecules* **1989**, *22*, 1946.
- Durand, D.; Naveau, F.; Busnel, J. P.; Delsanti, M.; Adam, M. *Macromolecules* **1989**, *22*, 2011.
- Wachenfeld-Eisele, E.; Burchard, W. *Macromolecules* **1989**, *22*, 2496.
- Lapp, A.; Leibler, L.; Schosseler, F.; Strazielle, C. *Macromolecules* **1989**, *22*, 2871.
- Adam, M.; Delsanti, M. *Contemp. Phys.* **1989**, *30*, 203.
- Adam, M.; Delsanti, M.; Munch, J. P.; Durand, D. *Physica A* **1990**, *163*, 85.
- Delsanti, M.; Munch, J. P.; Durand, D.; Busnel, J. P.; Adam, M. *Europhys. Lett.* **1990**, *13*, 697.
- Schosseler, F.; Daoud, M.; Leibler, L. *J. Phys. (Paris)* **1990**, *51*, 2373.
- Bauer, J.; Lang, P.; Burchard, W.; Bauer, M. *Macromolecules* **1991**, *24*, 2634.
- Adam, M.; Lairez, D.; Boue, F.; Busnel, J. P.; Durand, D.; Nicolai, T. *Phys. Rev. Lett.* **1991**, *67*, 3456.
- Stauffer, D. *Introduction to Percolation Theory*; Taylor & Francis: Philadelphia, PA, 1985.
- Daoud, M.; Bouchaud, E.; Jannink, G. *Macromolecules* **1986**, *19*, 1955.
- De Gennes, P. G. *Scaling Concepts in Polymer Physics*; Cornell University Press: Ithaca, NY, 1979; p 152.
- Isaacson, J.; Lubensky, T. C. *J. Phys. (Paris) Lett.* **1980**, *41*, L-469.
- Daoud, M.; Joanny, J. F. *J. Phys. (Paris)* **1981**, *42*, 1359.
- Daoud, M.; Lapp, A. *J. Phys. Condens. Matter* **1990**, *2*, 4021.
- Daoud, M.; Family, F.; Jannink, G. *J. Phys. (Paris) Lett.* **1984**, *45*, L-199.
- In practice it is difficult to distinguish logarithmic divergences from power laws with small exponents, which makes the intrinsic viscosity-weight-average molecular weight relation less useful for determining universality class.
- Wesson, J. A., unpublished, 1989.
- Furniss, B. S.; Hannaford, A. J.; Rogers, V.; Smith, P. W. G.; Tatchell, A. R. *Vogel's Textbook of Practical Organic Chemistry*; Longman: Essex, England, 1978.
- Mourey, T. H.; Miller, S. M.; Balke, S. T. *J. Liq. Chromatogr.* **1990**, *13*, 435.
- Mourey, T. H.; Miller, S. M. *J. Liq. Chromatogr.* **1990**, *13*, 693.
- Mourey, T. H.; Miller, S. M.; Wesson, J. A.; Long, T. E.; Kelts, L. W. *Macromolecules* **1992**, *25*, 45.
- Mourey, T. H.; Turner, S. R.; Rubinstein, M.; Frechet, J.; Hawker, C.; Wooley, K. *Macromolecules* **1992**, *25*, 2401.
- Hamiel, A. E.; Ouano, A. C. *J. Liq. Chromatogr.* **1978**, *1*, 111.
- Whitney, R. S.; Burchard, W. *Makromol. Chem.* **1980**, *181*, 869.
- Trappe, V.; Burchard, W.; Steinmann, B. *Makromol. Chem.* **1991**, *45*, 63.
- Panyukov, S. V. *Sov. Phys.—JETP (Engl. Transl.)* **1990**, *71*, 372.
- Patel, S. K.; Malone, S.; Cohen, C.; Gillmor, J. R.; Colby, R. H. *Macromolecules* **1992**, *25*, 5241.
- Ma, S.-K. *Modern Theory of Critical Phenomena*; Benjamin/Cummings: Reading, MA, 1976.
- Rubinstein, M.; Colby, R. H.; Gillmor, J. R. In *Space-Time Organization in Macromolecular Fluids*; Tanaka, F., Doi, M., Ohta, T., Eds.; Springer-Verlag: New York, 1989; p 66.
- Rubinstein, M.; Colby, R. H.; McLeish, T. C. B. In *Extended Abstracts—Fractal Aspects of Materials*; Kaufman, J. H., Martin, J. E., Schmidt, P. W., Eds.; Materials Research Society: Pittsburgh, PA, 1989; p 239.
- Colby, R. H.; Gillmor, J. R.; Rubinstein, M., manuscript in preparation.